Dissipative dynamics in a finite chaotic environment: Relationship between damping rate and Lyapunov exponent

J. C. Xavier,[1,2] W. T. Strunz,[2] and M. W. Beims[1,3]
[1]*Departamento de Física, Universidade Federal do Paraná, 81531-980 Curitiba, Brazil*
[2]*Institut für Theoretische Physik, Technische Universität Dresden, D-01069 Dresden, Germany*
[3]*Max Planck Institute for the Physics of Complex Systems, Nöthnitzer Strasse 38, D-01187 Dresden, Germany*
(Received 24 March 2015; revised manuscript received 4 June 2015; published 17 August 2015)

We consider the energy flow between a classical one-dimensional harmonic oscillator and a set of N two-dimensional chaotic oscillators, which represents the finite environment. Using linear response theory we obtain an analytical effective equation for the system harmonic oscillator, which includes a frequency dependent dissipation, a shift, and memory effects. The damping rate is expressed in terms of the environment mean Lyapunov exponent. A good agreement is shown by comparing theoretical and numerical results, even for environments with mixed (regular and chaotic) motion. Resonance between system and environment frequencies is shown to be more efficient to generate dissipation than larger mean Lyapunov exponents or a larger number of bath chaotic oscillators.

DOI: 10.1103/PhysRevE.92.022908 PACS number(s): 05.45.−a, 05.90.+m, 05.20.−y, 05.40.−a

I. INTRODUCTION

Realistic physical systems are usually not isolated but they continuously interact with their surroundings (the environment). The kind of interaction between the system and environment, and the dynamics of the environment itself, determine the dissipative dynamics of the open system. In fact, the Brownian motion, which is the motion of a free particle coupled to an environment, is a first example of such open systems and was described a long time ago [1–4]. Indeed, Langevin [4] described the Brownian motion by using the stochastic differential equation (the Uhlenbeck-Ornstein process)

$$\frac{dv}{dt} = -\gamma v + \xi(t), \tag{1}$$

where v is the velocity of the particle in a fluid. The first term on the right side is the friction with damping rate γ, $\xi(t)$ is a rapidly varying force due to the collisions of the surrounding fluid molecules. The force $\xi(t)$ can be conveniently considered as a Gaussian noise with vanishing mean value and correlation function that obeys

$$\langle \xi(t)\xi(t')\rangle = 2D\delta(t-t'). \tag{2}$$

The brackets represent an average over the distribution of an ensemble of realizations of the fluctuating force and D is the diffusion coefficient. The temperature of the Brownian particle is defined by the fluctuation-dissipation relation, such that $D = \gamma k_B T/m$ (m is the mass of the particle) provides a way to introduce both fluctuations and irreversibility in a simple form. In this case the averaged initial energy of the Brownian particle decays exponentially in time with 2γ.

When more complicated systems are considered, the specific choice of the environment (or bath) is certainly of most relevance for the system dissipation process. One often uses a model where dissipation in quantum systems is described by a system of interest coupled bilinearly to a set of noninteracting harmonic oscillators (HOs) with a continuous linear frequency distribution [5]. It can be shown, that for such a model the motion of the system is governed by *generalized* Langevin equations (classical and quantum) in the limit case of an infinite-size heat bath [6]. The word *generalized* refers to the explicit appearance of the memory integral involving a non-Markovian dynamics. In the classical case the usual fluctuation-dissipation relation is obtained. Thus, the presumption of an infinite number of linear HOs in the heat bath permits irreversible energy flow into the bath, and leads to solutions with Boltzmann energy distribution for the central system, i.e., thermalization at the bath temperature. However, the presence of an infinite number of a continuous distribution of frequencies of the oscillators may not always be justified. There are many physical situations where the environment is composed by a finite number of constituents. In such cases the bath itself can be highly structured, containing specific modes which strongly influence the system dynamics. As examples of finite baths we mention nanoscale devices [7], single localized spin 1/2 coupled to a finite spin-polarized environment [8], superconducting quantum bit coupled to an environment composed of a single electromagnetic mode of the cavity [9], and the energy transfer between a light-harvesting protein and a reaction center protein [10]. The first attempt to theoretically describe a finite environment composed of HOs was realized by [11]. In general the behavior of the main system due to the finite bath may change drastically [7,12–16]. Moreover, when kicked HOs are used for the bath, the usual fluctuation-dissipation relation is not valid anymore, memory effects are present and the dissipation process can be very complex [17].

Another way to describe the interaction of the system and environment is to consider the bath composed by a low-dimensional chaotic system [18]. This was first analyzed by Wilkinson [19] and Berry and Robbins [20], showing that the rate of energy exchange between the slow system and the fast chaotic bath in a microcanonical ensemble of realizations, drastically depends on the classical motion of the bath constituents. The rate of energy exchange increases when the environment exhibits chaotic motion. In these works they use the notion of adiabatic invariants of the chaotic energy shell, proposed by Ott [21] and Brown *et al.* [22]. This formalism gives in first order a Born-Oppenheimer

reaction force, followed by a force proportional to the system velocity [20]. The velocity dependent force splits into a "magnetic" and a "deterministic" friction which produces energy flow from the system to the bath, hereafter named dissipation. The friction force evolves the slow degrees of freedom towards a state of statistical equilibrium with the fast degrees [23,24], but these distributions may not be of Boltzmann-like type. This occurs because the systems are small and they may depend on the density of states of the involved systems and initial conditions (ICs) [25–27]. The Boltzmann-like distribution only occurs when the number of chaotic degrees of freedom in the bath is increased (but still finite), such that even for a single realization it is possible to see irreversible processes [28].

The purpose of the present work is to study dissipation of a HO coupled to a finite number of chaotic environments, modeled by two-dimensional quartic oscillators (QOs). The main idea is to write down an effective equation of motion for the HO which includes analytical expressions containing information from the bath. Our goal is not to discuss thermostatting mechanisms, which could be somehow related to the present work. We use the Linear Response Theory (LRT) to evaluate the nonequilibrium distribution function following the approach presented in Ref. [28]. We show that the effective damping rate depends on the HO and QOs frequencies, Lyapunov exponent (LE) from the QOs, and time-dependent memory effects which disappear for larger times. In addition, we make a direct connection of the damping rate obtained for a collection of QOs with the spectral density obtained for one QO [18]. Even though larger LEs from the bath tend to increase the damping rates, a resonance between the HO effective frequency and bath frequency are more effective to generate larger dissipation.

Our work is presented in the following manner. In Sec. II we describe the system-environment model and discuss its relevant dynamics. In Sec. III our results are shown and discussed. This includes the use of the LRT to derive the effective system equation, and the numerical and analytical determination of the damping rate. Section IV summarizes our main results.

II. THE MODEL

The starting point for our analysis is the classical Hamiltonian

$$H = H_S + H_B + H_I, \tag{3}$$

which consists of three parts H_S, H_B, and H_I, which correspond to the system, environment (or bath), and the interaction, respectively. The Hamiltonians are described by [28]

$$H_S = \frac{p^2}{2m} + \frac{m\omega_0^2 q^2}{2}, \tag{4}$$

$$H_B = \sum_{i=0}^{N} \frac{p_{x_i}^2 + p_{y_i}^2}{2} + \frac{a\left(x_i^4 + y_i^4\right)}{4} + \frac{x_i^2 y_i^2}{2}, \tag{5}$$

$$H_I = \sum_{i=0}^{N} \lambda_N x_i q. \tag{6}$$

The system, with generalized coordinates (q, p), describes a particle of mass m subjected to a one-dimensional HO with angular frequency ω_0. The bath is composed of a finite sum of two-dimensional QO, and the ith particle in the environment is characterized by the generalized coordinates ($\vec{q}_i = x_i\hat{\imath} + y_i\hat{\jmath}$, $\vec{p}_i = p_{x_i}\hat{\imath} + p_{y_i}\hat{\jmath}$). The interaction between the bath and the system is described by a bilinear coupling, where $\lambda_N = \lambda/\sqrt{N}$ is a measure of the effective coupling, allowing the comparison of results obtained for different values of N [28].

Some words about the properties of the model are in order. The total Hamiltonian (3) is conservative, but due to energy exchanges between system and environment, the system behaves dissipatively [24,28]. The nonlinear dynamics of the bath is independent of the QOs energy $H_B = E_B$, but is completely controlled by the parameter a. It is integrable for $a = 1.0$, strongly chaotic for $a = 10^{-3}$, and mixed for intermediate values of a. While we focus our analytical results on the system dynamics, we compare them with the results obtained by solving numerically the $4N + 2$ equations of motion related to the Hamiltonians (4), (5), and (6). For the case $N = 1$ and $a = 0.1$, it is possible to show [24] that, in an ensemble of realizations, the fast low-dimensional chaotic dynamics of the environment acts as a sink of energy for the system. System and bath reach an equilibrium state which is not necessarily a Boltzmann-like distribution. A temperature for this case can only be defined by modifying the definition of entropy [29,30]. A theoretical description based on the LRT [31] allows for a description of the system energy decay for short times, and does not give information about long time behaviors. It only provides, based on the initial system and bath energy, some necessary conditions to promote dissipation.

The QOs are not directly coupled to each other, but are indirectly coupled via the system. When the number of QOs increases [28], the indirect and weak interaction between the QOs plays a fundamental role in the system dynamics. It allows for the observation of equilibration and dissipation. Fixing the number of QOs, it is possible to study the influence of the chaotic motion to promote dissipation. For $N = 100$, for example, the time dependence of the energy of the system $E_S(t)$ changes qualitatively for distinct values of a. In the integrable regime, $a = 1.0$, $E_S(t)$ decreases a small amount from its initial value $E_S(0)$, and tiny oscillations around its mean value are observed. Similar results are obtained in the mixed regime, but in this case the mean value of the energy $[\overline{E}_S(t)]$ is lower, and the oscillations slightly larger. For the strongly chaotic case, $a = 0.01$, the energy decay is exponential, $E_S(t) = E_S(0)e^{-\gamma t}$, with γ being a function of the bath properties and the frequency of the system. These results remain valid for a single realization, as long as N is large [28]. This strongly differs from the case $N = 1$, where 10^3 trajectories are necessary [24]. The number of degrees of freedom in the chaotic bath is important as well. When N is small ($N \lesssim 100$), $E_S(t)$ fluctuates and it is not possible to see the exponential decay mentioned above. For larger values of $N(\gtrsim 100)$, $E_S(t)$ continues to decay exponentially and γ becomes independent of N [28]. Another important feature observed for large values of N, is that the system thermalizes with the environment and it is possible to define a temperature since the equilibrium energy distribution is a Boltzmann-like distribution. This property has not been observed when the

bath is in a regular or mixed regime, independently of N. Therefore, irreversible processes may occur when the bath is composed by large values of $N(\gtrsim 100)$ and the QOs having a chaotic dynamics.

In this context, up to now the theoretical description developed for system interacting with a finite number ($N > 1$) of chaotic baths [28] only considers the effects of the initial bath temperature, and does not include the system frequency. In all simulations in this paper we will use for the system $m = 1$, $q(0) = 0$, $p(0) = \sqrt{2mE_S(0)}$, $E_S(0) = 10.0$, and $\lambda = 0.01$. The equations of motions are solved numerically using a fourth-order Runge-Kutta integrator [32] with fixed step $\Delta t = 10^{-3}$.

III. RESULTS

A. Equation of motion for the system

Hamilton's equation of motion for the system is

$$\ddot{q} + \omega_0^2 q = -\frac{\lambda_N}{m} X(t), \tag{7}$$

where

$$X(t) = \sum_{i=1}^{N} x_i. \tag{8}$$

Supposing that the environment oscillators behave chaotically, we may replace $X(t)$ by its average $\langle X(t)\rangle$, so that Eq. (7) can be rewritten as

$$\ddot{q} + \omega_0^2 q \approx -\frac{\lambda_N}{m}\langle X(t)\rangle. \tag{9}$$

In order to evaluate the average $\langle X(t)\rangle$, we use the LRT [31] following the steps and arguments proposed in Ref. [28], where more details about this subsection can be found. The key idea in this procedure is to consider the response of the bath due to a perturbation of the system.

The next step is to define a temperature for the environment before coupling it to the system, and for this we chose a Boltzmann-like distribution. It was observed numerically that after coupling the bath to the system we still have a Boltzmann-like distribution. Therefore

$$p\left(E_B^{(i)}\right) = \frac{1}{\bar{E}_B} e^{-E_B^{(i)}/\bar{E}_B} \tag{10}$$

is valid for long times. Here $E_B^{(i)}$ is the energy from Eq. (5), and $\bar{E}_B$ is the average energy of the bath which, after using the equipartition theorem, is given by $\bar{E}_B = \bar{H}_B = \bar{T} + \bar{V} = k_B T + k_B T/2 = 3k_B T/2$ [28]. It was considered that the distribution from Eq. (10) is obtained before the system-bath coupling is turned on. After straightforward calculation we get

$$\langle X(t)\rangle = \langle X(t)\rangle_e - \lambda_N \int_0^t \phi_{XX}(t-s) q(s) ds, \tag{11}$$

where the index e indicates that the average is taken over a canonical distribution of energy given by Eq. (10). We note that $\langle X(t)\rangle_e = \langle \xi(t)\rangle_e$ represents the stochastic contribution which appears in Eq. (1). In this approach we assume that the environmental energy is very small compared to the initial HO's energy. In other words, we consider a cold environment where thermal fluctuations after equilibration are negligible. Due to the parity of H_B we have $\langle X(t)\rangle_e = 0$, so that Eq. (11) results in

$$\langle X(t)\rangle = -\lambda_N \int_0^t \phi_{XX}(t-s) q(s) ds. \tag{12}$$

The average $\langle X(t)\rangle$ is a function of $\phi_{XX}(t-s)$, which is the response function of the bath due the system perturbation, and is given by

$$\phi_{XX}(t-s) = \left\langle \sum_{i=1}^{N} \frac{(t-s)}{4H_B^{(i)}} p_{x_i}(t) p_{x_i}(s) \right\rangle_e + \left\langle \sum_{i=1}^{N} \frac{5}{4H_B^{(i)}} x_i(t) p_{x_i}(s) \right\rangle_e, \tag{13}$$

or

$$\phi_{XX}(t-s) = \frac{5}{4}\frac{d}{ds} C_N(t-s) + \frac{(t-s)}{4}\frac{d^2}{dsdt} C_N(t-s) \tag{14}$$

with the correlation function

$$C_N(t-s) = \left\langle \sum_{i=1}^{N} \frac{x_i(t) x_i(s)}{E_B^{(i)}} \right\rangle_e. \tag{15}$$

Thus, the system's equation of motion becomes

$$\ddot{q} + \omega_0^2 q = \frac{\lambda_N^2}{m} \int_0^t \phi_{XX}(t-s) q(s) ds \tag{16}$$

which gives us the information about the harmonic motion of the system when it is coupled to a bath of N chaotic systems obeying the initial energy distribution. All relevant information about the bath is contained in the response function (14). As we will see, this function is responsible for the dissipative effects and gives rise to the damping rate, so that the right-hand side of Eq. (16) can be written as a velocity dependent friction, turning the system's equation of motion into an equation for the damped HO.

B. The response function and the energy decay

As pointed out before, numerical simulations show that the energy distribution of the bath, at equilibrium, is a Boltzmann-like distribution and it does not change so much from the initial distribution. When $\bar{E}_B(0) \ll E(0)$ (around 10% or less), the system energy decay is exponential and goes to zero for long times [28]. This allows us to interpret the system motion as a damped harmonic oscillator and to describe its motion based on this idea. Thus, we have to find a velocity dependent term in Eq. (16), whose coefficient will be responsible for the dissipative process. In order to do this, we write

$$\phi_{XX}(t-s) = \frac{5}{4}\frac{d}{ds} C_N(t-s) + \frac{(t-s)}{4}\frac{d^2}{dsdt} C_N(t-s), \tag{17}$$

where the second term on the right-hand side can be rewritten as

$$\frac{(t-s)}{4}\frac{d^2}{dsdt}C_N(t-s) = \frac{d}{ds}\left(\frac{(t-s)}{4}\frac{d}{dt}C_N(t-s) - \frac{1}{4}C_N(t-s)\right), \quad (18)$$

and we have used $\frac{dC_N}{ds} = -\frac{dC_N}{dt}$. Thus, Eq. (17) becomes

$$\phi_{XX}(t-s) = \frac{d}{ds}\left(C_N(t-s) + \frac{(t-s)}{4}\frac{d}{dt}C_N(t-s)\right),$$

and defining

$$\alpha(t-s) = C_N(t-s) + \frac{(t-s)}{4}\frac{d}{dt}C_N(t-s), \quad (19)$$

we finally have

$$\phi_{XX}(t-s) = \frac{d}{ds}\alpha(t-s). \quad (20)$$

Substituting Eq. (20) into Eq. (16), and doing the integral by parts, yields

$$\ddot{q} + \omega^2 q = -\frac{\lambda_N^2}{m}\int_0^t \alpha(t-s)\dot{q}(s)ds, \quad (21)$$

where we used $q(0) = 0$ and defined $\omega^2 = \omega_0^2 - \frac{\lambda_N^2}{m}\alpha(0)$. The right-hand side of Eq. (21) is now a dissipative term proportional to the velocity of the system, and $\alpha(t-s)$ is the memory kernel. In this way, memory properties which include information about the whole history of the trajectory until time t, are contained in the function $\alpha(t-s)$. We note that in the right-hand side of Eq. (21) a term proportional to $q(0)\,\alpha(t)$ was neglected by choosing $q(0) = 0$. This avoids an initial energy arising from the interaction. A first attempt to solve the integral on the right-hand side of Eq. (21), would be to consider a Markovian environment (no memory terms), for which we use the approximation $\alpha(t-s) \approx C\delta(t-s)$ [28]. However, such approximation leads to a dissipation constant which is independent of the system's frequency, which is not our case. To show this we display in Fig. 1 the system's energy decay dependence on the frequency. Thus, we expect that the memory term $\alpha(t-s)$ may also depend in some way on the frequency. In addition, the δ-function approximation assumes that $\alpha(t-s)$ does not change too much in the interval of time when the peak occurs. To check this in more details, the time behavior of $\alpha(t-s)$, which only depends on environmental variables, was obtained numerically from Eq. (19) and is plotted in Fig. 2. It is possible to see that it is a well-localized function around s, and that asymptotically the amplitude of this function is constant. The $s < 150$ values can be interpreted as a transient and will be neglected. In addition, it is visible that we can consider the same shape for $\alpha(t-s)$, independently of s. In our problem the velocity of the system oscillates many times while $\alpha(t-s)$ is relevant. Thereby, we need to transform variables in such a way that the system coordinates become practically constant in the interval of time for which $\alpha(t-s)$ is different from zero. Such new coordinates are named as slow coordinates, and the old ones as fast coordinates. Therefore,

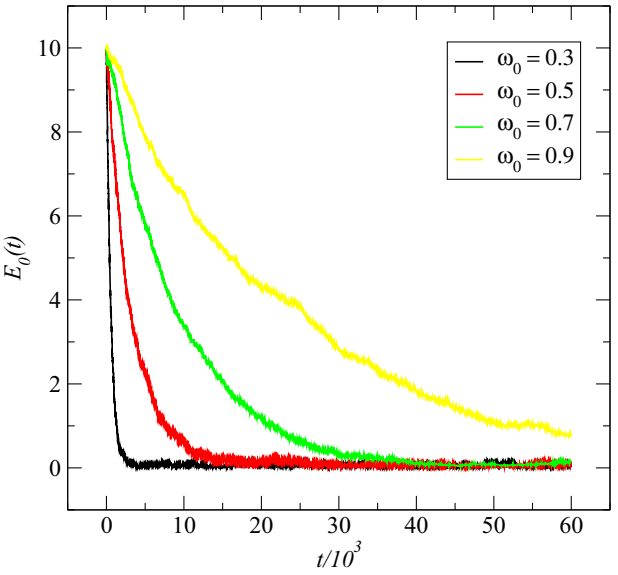

FIG. 1. (Color online) Average system energy decay for four realizations and different values of ω_0. The number of QOs in the bath is $N = 2000$ and $a = 10^{-3}$. The ICs for the QOs are chosen using the parametrization given in Ref. [24]. The small average is only to avoid fluctuations due the choice of ICs.

we write Eq. (21) as a matrix,

$$\begin{pmatrix}\dot{q}(t)\\ \dot{p}(t)\end{pmatrix} = \Omega\begin{pmatrix}q(t)\\ p(t)\end{pmatrix} - \frac{\lambda_N^2}{m}\int_0^t \underline{\alpha}(t-s)\begin{pmatrix}q(s)\\ p(s)\end{pmatrix}ds \quad (22)$$

with

$$\underline{\alpha}(t-s) = \begin{pmatrix}0 & 0\\ 0 & \alpha(t-s)\end{pmatrix}, \quad (23)$$

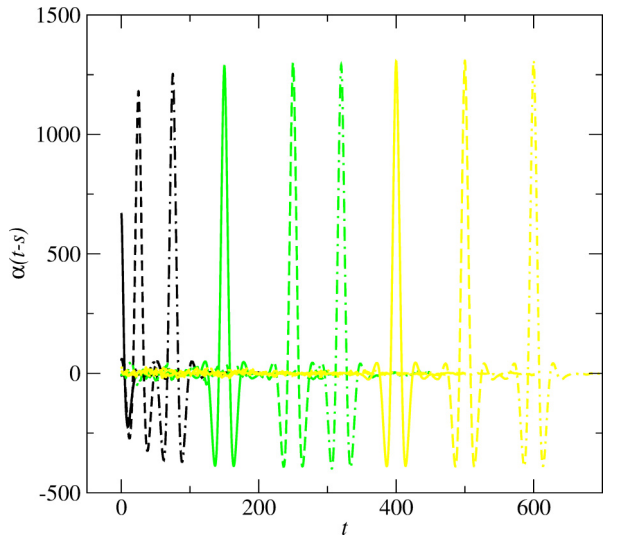

FIG. 2. (Color online) Plotted is the memory kernel, $\alpha(t-s)$, from Eq. (19), as a function of time for different values of s. The average in Eq. (19) is over 10^5 realizations with an initial energy distribution given by Eq. (10), $a = 0.01$ and $\bar{E}_B = 0.1$. The ICs and energy distribution are the same as used in Fig. 1.

and

$$\Omega = \begin{pmatrix} 0 & \frac{1}{m} \\ -m\omega^2 & 0 \end{pmatrix}. \tag{24}$$

Now we introduce the slow coordinates

$$\begin{pmatrix} \tilde{q}(t) \\ \tilde{p}(t) \end{pmatrix} = e^{-\Omega t} \begin{pmatrix} q(t) \\ p(t) \end{pmatrix}, \tag{25}$$

and Eq. (22) becomes

$$\begin{pmatrix} \dot{\tilde{q}}(t) \\ \dot{\tilde{p}}(t) \end{pmatrix} = -\frac{\lambda_N^2}{m} \int_0^t e^{-\Omega t} \underline{\alpha}(t-s) e^{\Omega s} \begin{pmatrix} \tilde{q}(s) \\ \tilde{p}(s) \end{pmatrix} ds, \tag{26}$$

where $e^{-\Omega t}$ is the solution of the uncoupled HOs, given by

$$e^{-\Omega t} = \begin{pmatrix} \cos(\omega t) & -\frac{\sin(\omega t)}{m\omega} \\ m\omega \sin(\omega t) & \cos(\omega t) \end{pmatrix},$$

with $e^{\Omega t} = (e^{-\Omega t})^{-1}$. The slow variables are almost constant compared to the product $e^{-\Omega t}\underline{\alpha}(t-s)e^{\Omega s}$ and it is possible to write Eq. (26) as

$$\begin{pmatrix} \dot{\tilde{q}}(t) \\ \dot{\tilde{p}}(t) \end{pmatrix} = -\frac{\lambda_N^2}{m^2} \begin{pmatrix} \tilde{q}(t) \\ \tilde{p}(t) \end{pmatrix} \int_0^t e^{-\Omega t} \underline{\alpha}(t-s) e^{\Omega s} ds, \tag{27}$$

where the slow variables are now only dependent on t. Therefore

$$\begin{pmatrix} \dot{\tilde{q}}(t) \\ \dot{\tilde{p}}(t) \end{pmatrix} = \gamma_T(\omega,t) \begin{pmatrix} \tilde{q}(t) \\ \tilde{p}(t) \end{pmatrix}, \tag{28}$$

with

$$\gamma(\omega,t) = -\frac{\lambda_N^2}{m} \int_0^t e^{-\Omega t} \underline{\alpha}(t-s) e^{\Omega s} ds. \tag{29}$$

We are looking for a damped harmonic oscillator equation of motion and Eq. (29) is now responsible for the dissipation process. It includes the frequency of the system through the exponential terms containing the uncoupled harmonic oscillator solution. The integrals will provide us the relationship of the dissipation with the system and bath properties. Our next step is to use the transformation $u = t - s$ and write down Eq. (29) in matrix form:

$$\gamma(\omega,t) = \frac{\lambda_N^2}{m} \begin{pmatrix} \sin^2(\omega t) c_1(\omega,t) - c_2(\omega,t) \sin(\omega t)\cos(\omega t) & -\frac{c_1(\omega,t)\sin(\omega t)\cos(\omega t)}{m\omega} - \frac{c_2(\omega,t)\sin^2(\omega t)}{m\omega} \\ -c_1(\omega,t)\, m\omega \, \sin(\omega t)\cos(\omega t) + c_2(\omega,t)\, m\omega \, \cos^2(\omega t) & c_1(\omega,t)\cos^2(\omega t) + c_2(\omega,t)\sin(\omega t)\cos(\omega t) \end{pmatrix},$$

with

$$c_1(\omega,t) = -\int_0^t du\, \alpha(u)\cos(\omega u), \tag{30}$$

and

$$c_2(\omega,t) = -\int_0^t du\, \alpha(u)\sin(\omega u), \tag{31}$$

Using Eqs. (28) and (25), it is now possible to go back to the fast coordinates, and write the system's equation of motion as

$$\ddot{q} - \gamma_T \dot{q} + \Omega_T^2 q = 0, \tag{32}$$

where

$$\gamma_T(\omega,t) = \frac{\lambda_N^2 |c_1(\omega,t)|}{m} \tag{33}$$

is the *theoretical damping rate* which depends, via Eq. (30), on the history of the trajectory from time $t = 0$ to time t. In addition we have the theoretical effective system frequency

$$\Omega_T^2 = \omega^2 + \frac{|c_2(\omega,t)|\omega\lambda_N^2}{m}. \tag{34}$$

The extra term inside Ω_T^2, proportional to $c_2(\omega,t)$, is an additional shift in the system energy due the bilinear coupling. However, in our case this term has frequency and also memory dependences via $c_2(\omega,t)$. The numerical and analytical determination of $\gamma_T(\omega,t)$ will be performed in the next two subsections.

C. The numerical solution for $\gamma_T(\omega)$

The integral (30) can be solved numerically if we consider the symmetry properties and the general behavior of $\alpha(t-s)$. The shape of $\alpha(t-s)$ from Fig. 2 is independent if we use s or t fixed. In fact, we can write $\alpha(t-s) = f(t)\, g(t-s)$, where $f(t)$ describes the peak of $\alpha(t-s)$ and tends to a constant for large times. On the other hand, $g(t-s)$ is a function which always has the same behavior, independent of the chosen t value. This can be observed in Fig. 2, where $\alpha(t-s)$ keeps its shape for $t > 150$. Times $t < 150$ are called transient times and are not considered here. Changing $u = t - s$ in Eq. (30) and doing the integral in s, the part responsible for the asymptotic behavior goes out of the integration and we only have one integral from zero to t, of the t independent part. The result of the integral will be the area under the integrating function. Thus, our results are valid for long times.

Now we are able to compute numerically the integral (30). Using $t = 300$, $a = 10^{-3}$, and an initial energy distribution given by Eq. (10), with $\bar{E}_B(0) = 0.1$ we compute the $\alpha(t-s)$ function over 10^5 realizations and a bath of $N = 2000$ QOs. This result is multiplied by $\cos[\omega(t-s)]$ and the area below the curve calculated when s goes from 0 to 300. This allows us to compute $\gamma_T(\omega,t)$ from Eq. (33). This is shown in Fig. 3(a) and is compared to γ_n from the exponential fit

$$\bar{E}_S(t) = [\bar{E}_S(0) - \bar{E}_S(50000)]e^{-\gamma_n t} + \bar{E}_S(50000), \tag{35}$$

where $\bar{E}_S(50000) \sim 0.07$. Equation (35) is the system energy decay obtained from the numerical integration of the full problem. Both results are in good agreement. The total mean energy after equilibrium is shared between the system and bath degrees of freedom, namely $\bar{E}_{\rm tot}(50000) = \bar{E}_S(50000) + N\bar{E}_B(50000)$. Since the whole problem is conservative, we have $\bar{E}_{\rm tot}(0) = \bar{E}_{\rm tot}(50000)$,

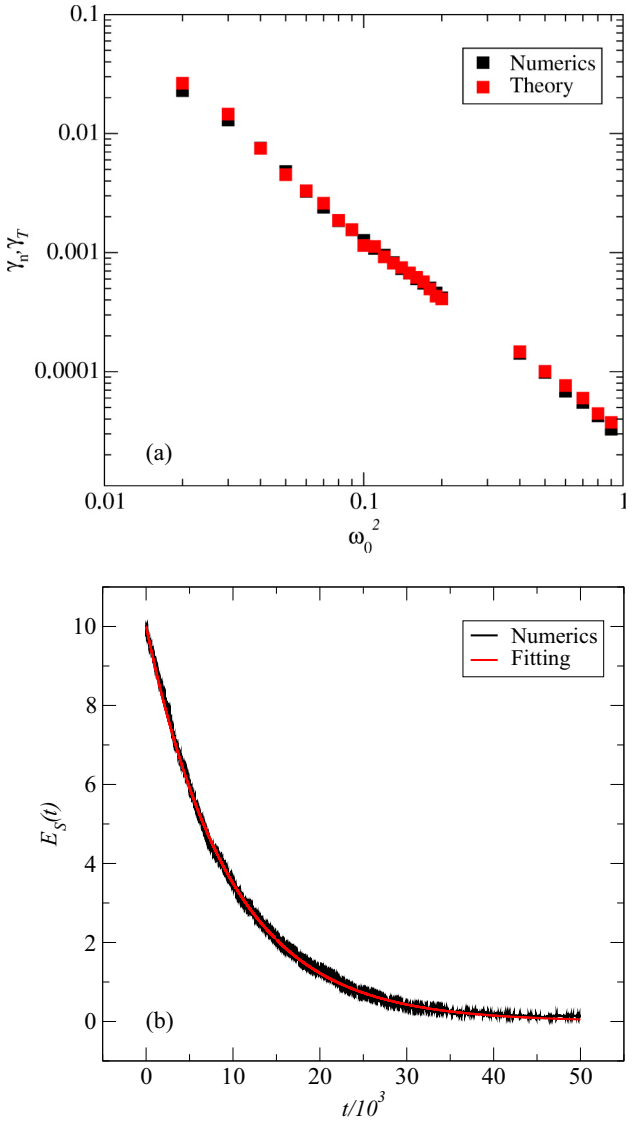

FIG. 3. (Color online) (a) Theoretical [$\gamma = \gamma_T(\omega, t = 300)$] and numerical ($\gamma = \gamma_n$) damping rates as a function of ω_0^2. (b) Numerical and exponential energy decays for $\omega_0 = 0.3$. The numerical values were obtained using an average over ten realizations.

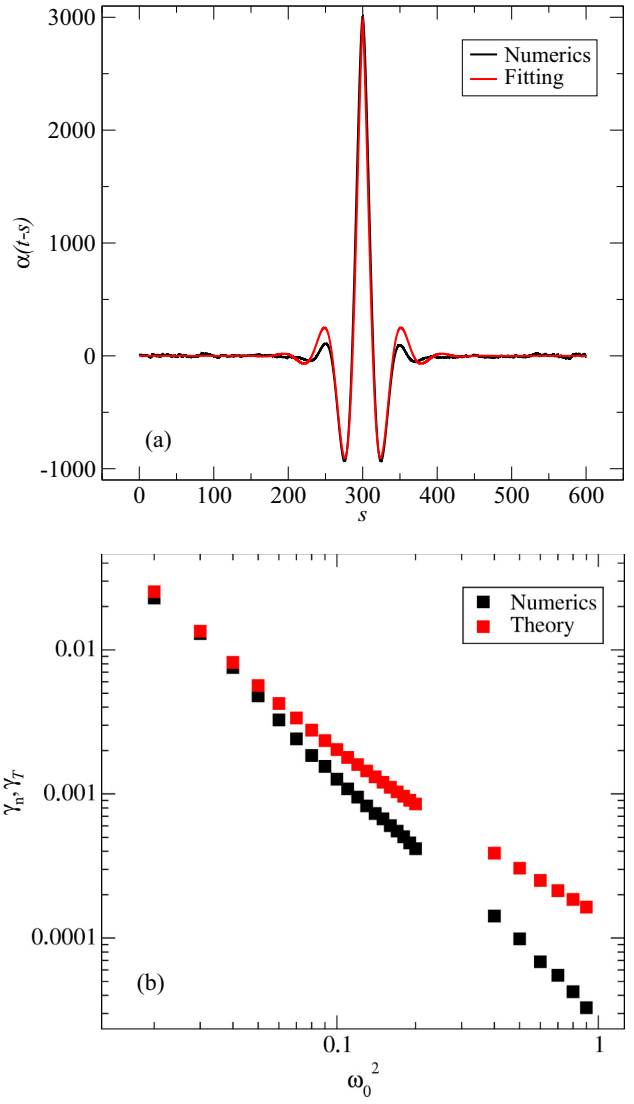

FIG. 4. (Color online) (a) Function $\alpha(t - s)$ obtained using Eq. (19) and the curve (36). (b) Theoretical [$\gamma = \gamma_T(\omega)$] and numerical ($\gamma = \gamma_n$) as a function of ω_0^2 for $N = 2000$ and $a = 10^{-3}$. For the fitting curve we used $\mu = 3.009$, $\omega_B = 0.115$, and $\sigma = 0.0470597$.

and using the energy equipartition theorem we can write $\bar{E}_S(0) + N\bar{E}_B(0) = k_BT + \frac{3}{2}Nk_BT$, which allows us to determine the equilibrium temperature from $k_BT = 2[\bar{E}_S(0) + N\bar{E}_B(0)]/(2 + 3N)$. Using $\bar{E}_S(0) = 10.0, \bar{E}_B = 0.1$, and $N = 2000$ we obtain $k_BT = 0.07$. From this we can also calculate $\bar{E}_S(50000) = k_BT = 0.07$ and $\bar{E}_B(50000) = \frac{3}{2}k_BT = 0.105$, which is nicely rewritten as $\bar{E}_B(50000) = \bar{E}_B(0) + \bar{E}_S(0)/2000$.

Figure 3(b) shows the system energy decay obtained from the numerical solution of the Hamiltonian (3), compared to an exponential decay using Eq. (33). From Figs. 3(a) and 3(b) we see that the analytical solution γ_T is in complete agreement with the numerical damping rate γ_n. This allows us to conclude that the transient behavior of the $\alpha(t - s)$ function is really not relevant to study energy decays, justifying the used approximation.

D. The analytical solution for $\gamma_T(\omega)$

The well-defined shape of $\alpha(t - s)$ in Fig. 2, and its independence on s, motivated us to find an approximated analytical function to describe it. This function is given by

$$\alpha(t - s) = \mu e^{-|t-s|/\sigma} \cos[\omega_B(t - s)], \tag{36}$$

where μ,σ, and ω_B are fit parameters to be determined. To check the validity of this function, Fig. 4(a) compares one specific example of both, $\alpha(t - s)$ obtained numerically from Eq. (19), and the adjusting curve (36). Thus, substituting Eq. (36) into Eq. (30), and calculating the integral, Eq. (33)

becomes

$$\gamma_T(\omega,t) \sim -\frac{\lambda_N^2\mu}{2\sigma\, m}\left(\frac{1}{\frac{1}{\sigma^2}+\Delta\omega_-^2}+\frac{1}{\frac{1}{\sigma^2}+\Delta\omega_+^2}\right)+\frac{\lambda_N^2\mu e^{-\frac{t}{\sigma}}}{2\,m}$$
$$\times\left\{\frac{1}{\frac{1}{\sigma^2}+\Delta\omega_-^2}\left(\frac{\cos(\Delta\omega_-)t}{\sigma}-\Delta\omega_-\sin(\Delta\omega_-)t\right)\right.$$
$$\left.+\frac{1}{\frac{1}{\sigma^2}+\Delta\omega_+^2}\left(\frac{\cos(\Delta\omega_+)t}{\sigma}-\Delta\omega_+\sin(\Delta\omega_+)t\right)\right\},$$

where $\Delta\omega_- = \omega-\omega_B$ and $\Delta\omega_+ = \omega+\omega_B$. Interesting to observe here is that the time dependence of $\gamma_T(\omega,t)$ decays as fast as the memory kernel from Eq. (36). Therefore the initial time oscillations of the damping rate are related to non-Markovian properties of the chaotic environment. Here ω_B gives the fastness of the chaotic motion. For larger times we obtain

$$\gamma_T(\omega) \approx -\frac{\lambda_N^2\mu}{2\sigma m}\left(\frac{1}{\frac{1}{\sigma^2}+\Delta\omega_-^2}+\frac{1}{\frac{1}{\sigma^2}+\Delta\omega_+^2}\right). \quad (37)$$

Figure 4(b) shows the asymptotic theoretical damping rate, Eq. (37), and the damping rate γ_n from the numerical simulations, as a function of the system's frequency. Disagreements are only observed for higher frequencies. This fact is related to the shape of the function chosen for the fitting curve, and its precision to describe the numerical function $\alpha(t-s)$. For times $t \gtrsim 1/\gamma_T(\omega)$, thermal equilibrium is reached with a small temperature ($k_BT \sim 0.07$). This small temperature also explains why the fluctuations in Fig. 1 are small after equilibrium.

Interesting to note is that expression (37) is, besides some constants, equal to the spectral density $S(\omega)$ obtained by fitting the correlation function for *one* chaotic environment [18]. While in that case it was not possible to give a closed expression for the damping rate, our procedure allows to obtain the dissipation coefficient for the HO coupled to N chaotic baths as

$$\gamma_T(\omega) = -\frac{\lambda_N^2}{4\,m}S(\omega). \quad (38)$$

This gives a direct connection between the spectral density of the chaotic environment and the damping rate. In a similar way it is possible to determine

$$c_2(\omega,t) \sim -\frac{\mu}{2}\left(\frac{\Delta\omega_-}{\frac{1}{\sigma^2}+\Delta\omega_-^2}+\frac{\Delta\omega_+}{\frac{1}{\sigma^2}+\Delta\omega_+^2}\right)+\frac{\mu e^{-\frac{t}{\sigma}}}{2}$$
$$\times\left\{\frac{1}{\frac{1}{\sigma^2}+\Delta\omega_-^2}\left(\Delta\omega_-\cos(\Delta\omega_-)t+\frac{\sin(\Delta\omega_-)}{\sigma}t\right)\right.$$
$$\left.+\frac{1}{\frac{1}{\sigma^2}+\Delta\omega_+^2}\left(\Delta\omega_+^2\cos(\Delta\omega_+)t+\frac{\sin(\Delta\omega_+)t}{\sigma}\right)\right\}$$

which for long times results in

$$c_2(\omega) \approx -\frac{\mu}{2}\left(\frac{\Delta\omega_-}{\frac{1}{\sigma^2}+\Delta\omega_-^2}+\frac{\Delta\omega_+}{\frac{1}{\sigma^2}+\Delta\omega_+^2}\right).$$

When this solution is substituted in Eq. (34) we obtain the frequency dependent shift.

E. Dissipation and the environment Lyapunov exponent

In Hamiltonian systems like Eq. (3), Lyapunov exponents (LEs) come in pairs and the sum of them must be zero [33]. Each environment QO has four LEs and, in the chaotic case, only one of them is positive. The goal of the present subsection is to understand how the damping rate from Eq. (37) depends on the positive LE from the environment (or on the parameter a). This brings us to an additional description of the dissipation, which includes an environment with mixed dynamics.

To do so, we first have to determine the a and N dependence of the three parameters μ,σ, and ω_B which appear in Eq. (37). This is shown in Fig. 5. The only parameter which changes with the N elements is μ. Thus, we can write

$$\mu = N\mu_1, \quad (39)$$

where μ_1 is the amplitude of $\alpha(t-s)$ for $N=1$. Figure 5(b) shows the dependence of μ_1, σ, and ω_B as a function of the parameter a. It is therefore possible to use a power law fit for these curves, namely

$$\mu_1(a) = \rho_\mu a^{-\phi_\mu}, \quad (40)$$
$$\sigma(a) = \rho_\sigma a^{-\phi_\sigma}, \quad (41)$$
$$\omega_B(a) = \rho_{\omega_B} a^{\phi_{\omega_B}}, \quad (42)$$

where $\rho_\mu = 3.265$, $\phi_\mu = 0.3266$, $\rho_\sigma = 3.670$, $\phi_\sigma = 0.2326$, $\rho_{\omega_B} = 0.6485$, and $\phi_{\omega_B} = 0.2612$. Now, using Eqs. (40)–(42), it is possible to write Eq. (37) as

$$\gamma_T(a) = -\frac{\lambda^2\rho_\mu}{2m^2\rho_\sigma a^{(\phi_\mu-\phi_\sigma)}}$$
$$\times\left(\frac{1}{\frac{a^{2\phi_\sigma}}{\rho_\sigma^2}+(\omega-\rho_{\omega_B}a^{\phi_{\omega_B}})^2}+\frac{1}{\frac{a^{2\phi_\sigma}}{\rho_\sigma^2}+(\omega+\rho_{\omega_B}a^{\phi_{\omega_B}})^2}\right), \quad (43)$$

which gives the relation of the damping rate with the chaoticity parameter a.

The next step is to write the parameter a as a function of the LEs from the environment. To simplify our analysis we consider the LEs from one uncoupled QO from the environment. It is obvious that for the whole coupled system and environment the LEs may change a small amount. We start computing the average LEs spectrum as a function of a using the Gram-Schmidt reorthonormalization procedure [34]. The result is shown in Fig. 6(a). We notice here that the energy flow from the system to the environment only occurs when the bath is in a chaotic regime, that is, when $0.0 \lesssim a \lesssim 0.3$. As already mentioned, we have at least one positive LE. Thus, we will focus in this range of a, describing a fitting for the mean positive LE, ($\langle\Lambda\rangle$). Using a piecewise function for the range of interest, we obtained four regimes $\mathbf{R_i}$ ($i = 1,\ldots,4$) with the

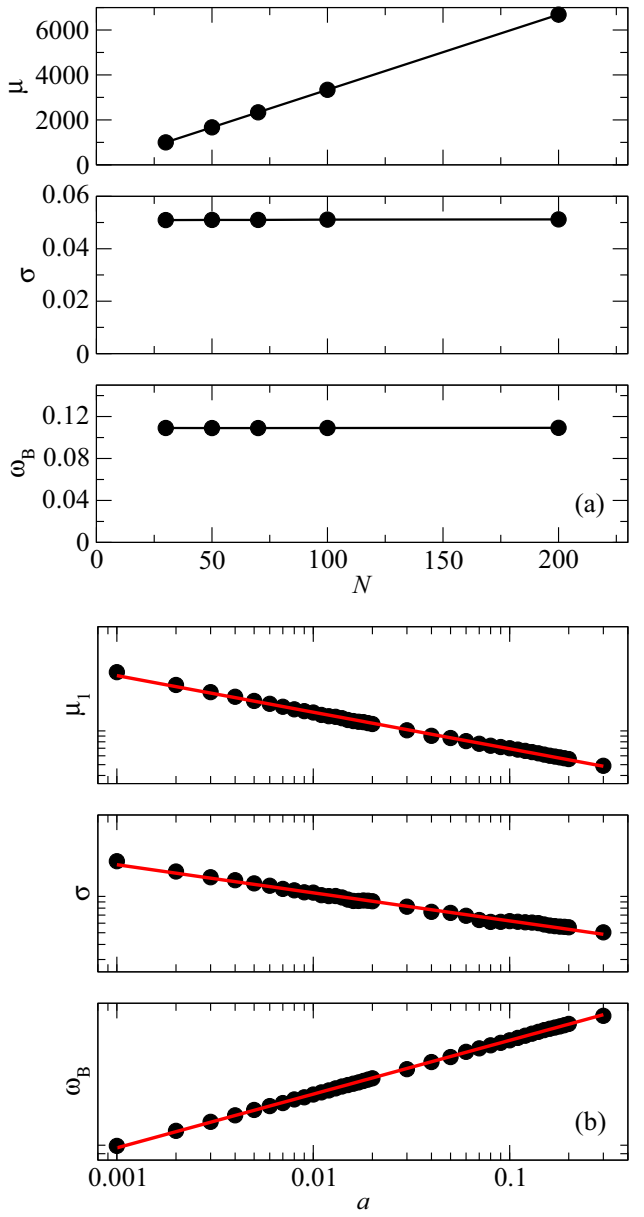

FIG. 5. (Color online) The fitting parameters μ, σ, and ω_B as a function of (a) N for $a = 10^{-3}$ and (b) a for $N = 1$. The black circles are the data from the fitting curve (36) for $\alpha(t - s)$, and the red (gray) line a power-law fit for the parameters. The initial energy distribution is given by Eq. (10) with $\bar{E} = 0.1$.

corresponding fitting curves

$$\langle\Lambda\rangle = \begin{cases} \xi_1 - \eta_1\, a^{\delta_1}, & \mathbf{R_1} : 10^{-3} < a \leqslant 0.007 \\ \xi_2 - \eta_2\, a^{\delta_2}, & \mathbf{R_2} : 0.007 < a \leqslant 0.11 \\ \xi_3 - \eta_3\, a^{\delta_3}, & \mathbf{R_3} : 0.11 < a \leqslant 0.27 \\ \eta_4\, e^{\delta_4 a}, & \mathbf{R_4} : 0.27 < a \leqslant 0.32 \end{cases}, \tag{44}$$

where $\xi_1 = 0, \eta_1 = -0.2982$, $\delta_1 = 0.007734$, $\xi_2 = 0.2924$, $\eta_2 = 0.7516, \delta_2 = 1$, $\xi_3 = 0.3514$, $\eta_3 = 0.1265, \delta_3 = 1$, $\eta_4 = 2.08838 \times 10^{12}$, and $\delta_4 = 122.4$. These fitting curves reproduce quite well the behavior of the mean LE, as can be checked in Fig. 6(b). Finally, inverting Eqs. (44) and substituting the result in $\gamma_T(a)$, we obtain the relation between the dissipation

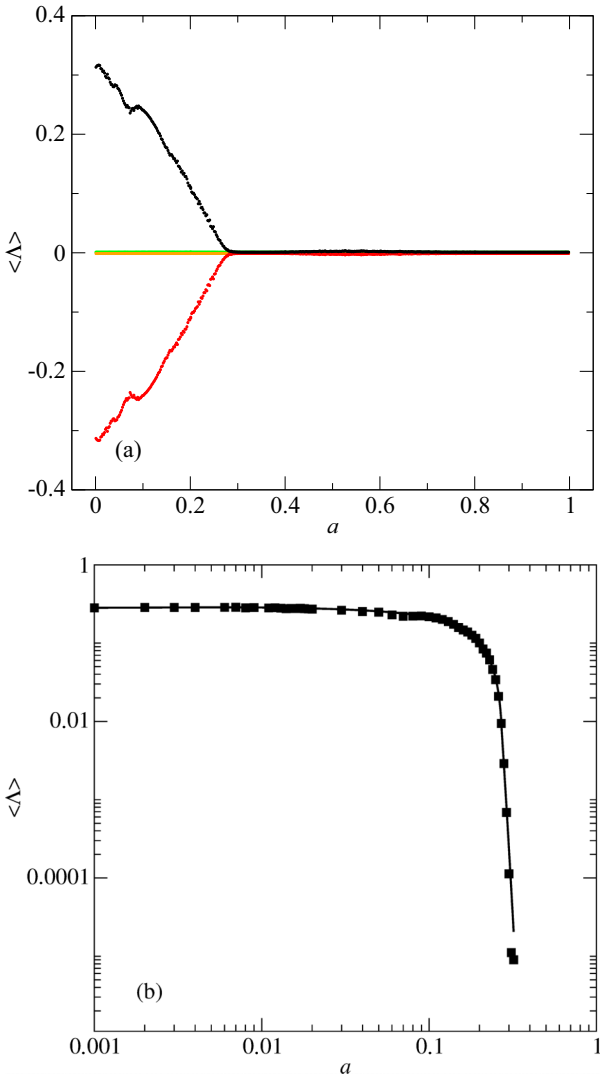

FIG. 6. (Color online) (a) Lyapunov spectrum for the QO as a function of a. The initial energy distribution is the same as used in Fig. 5. (b) Mean largest Lyapunov exponent (black square) and the corresponding fits from Eq. (44) (continuous lines).

and the mean largest LE. For the regimes $\mathbf{R_i}$ Eq. (37) becomes

$$\gamma_T^{(i)}(\langle\Lambda\rangle) \approx A_i \left(\frac{1}{B_i + (\omega - C_i)^2} + \frac{1}{B_i + (\omega + C_i)^2} \right), \tag{45}$$

where

$$A_i = -\frac{\lambda^2 \rho_\mu}{2m\rho_\sigma} \left(\frac{\eta_i}{\xi_i - \langle\Lambda\rangle} \right)^{\left(\frac{\phi_\mu - \phi_\sigma}{\delta_i}\right)},$$

$$B_i = \frac{1}{\rho_\sigma^2} \left(\frac{\xi_i - \langle\Lambda\rangle}{\eta_i} \right)^{\frac{2\phi_\sigma}{\delta_i}},$$

$$C_i = \rho_{\omega_B} \left(\frac{\xi_i - \langle\Lambda\rangle}{\eta_i} \right)^{\frac{\phi_{\omega_B}}{\delta_i}},$$

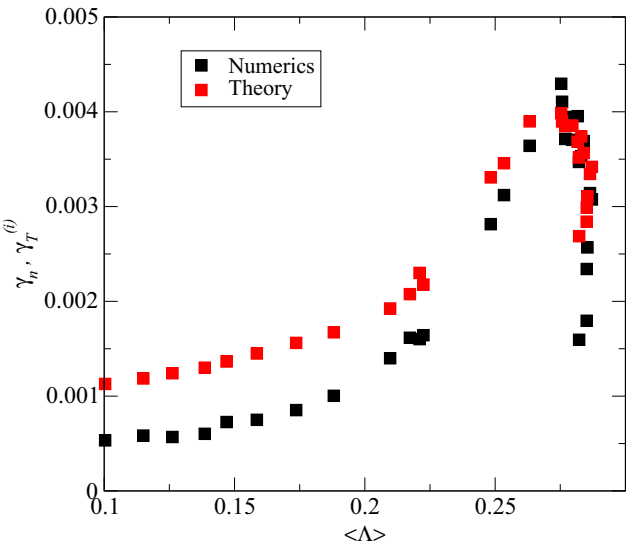

FIG. 7. (Color online) Comparison of the theoretical expression for the damping rates $\gamma_T^{(i)}$ with the damping rate γ_n. The numerical values were obtained using an average over ten realizations.

for $i = 1,2,3$, and

$$A_i = -\frac{\lambda^2\rho_\mu}{2m\rho_\sigma}\left[\frac{\delta_4}{\ln\left(\frac{\eta_4}{\langle\Lambda\rangle}\right)}\right]^{(\phi_\mu-\phi_\sigma)},$$

$$B_i = \frac{1}{\rho_\sigma^2}\left[\frac{\ln\left(\frac{\eta_4}{\langle\Lambda\rangle}\right)}{\delta_4}\right]^{2\phi_\sigma},$$

$$C_i = \frac{\rho_{\omega_B}}{\delta_4^{\phi_{\omega_B}}}\left[\ln\left(\frac{\eta_4}{\langle\Lambda\rangle}\right)\right]^{\phi_{\omega_B}},$$

for $i = 4$.

Figure 7 compares numerical and analytical results for the damping rates. Results are in remarkable agreement for larger values of the mean LE (strongly chaotic), where in general larger dissipation is observed. In this limit, we also observe a maximum of the dissipation coefficient which does not occur for the maximum LEs, but when the effective system frequency ω approaches the environment frequency ω_B. Close to the regular motion, where the LE approached zero, the dissipation decreases. From the analytical expressions for $\gamma_T^{(4)}(\langle\Lambda\rangle)$ we see that when $\langle\Lambda\rangle \to 0$, implies in $\gamma_T^{(4)}(\langle\Lambda\rangle) \to 0$. With our results, similar relations can be obtained between $\langle\Lambda\rangle$ and the spectral density $S(\omega)$ [18].

Additional simulations, not shown here, reveal that for larger a values, where a regular motion is obtained for the QOs, the fitting curve (36) still oscillates with frequency ω_B, but does not decays in time. In other words, σ becomes small and the damping rate $\gamma_T(\omega,t)$ oscillates for very long times.

IV. CONCLUSIONS

In this work we considered a one system harmonic oscillator coupled to an environment composed of a finite number N of quartic oscillators. By changing the control parameter, the dynamics of the quartic oscillators can be tuned from regular, mixed (coexistence of regular and chaotic) to chaotic motion. Using linear response theory and an appropriate description in terms of slow and fast coordinates, we were able to derive an effective equation for the system, Eq. (32), which includes shift and damping terms, both being time and frequency dependent. The time dependence of these quantities decays exponentially with the same rate as the memory kernel, and shows that, even for the strongly chaotic environment, a non-Markovian dynamics appears for short times. For a mixed environment, such non-Markovian effects tend to increase. In fact, this shows that even for a large number ($N \sim 2000$) of chaotic oscillators, some finite time memory effects are present. Our main result is an approximated analytical expression for the damping rate as a function of the system and environment frequencies, the environment nonlinear parameter a, and the mean positive Lyapunov exponent from the quartic oscillator. Extensive numerical simulations for the total system plus environment show a good agreement with our analytical results. The overall expected tendency is that the damping rate increases with the mean positive Lyapunov exponent from the environment. However, our analytical results show that the resonance between the system and environment is more efficient in generating larger damping rates. In addition, we found that the damping rate frequency dependence is identical to the spectral density obtained by fitting the correlation function for one chaotic environment [18].

Even though the analytical results of the present work can be used to see the effects for a bath with mixed (regular and chaotic) dynamics, a more precise description must be realized. Future investigations in this context will consider explicitly the effects of environments with a mixed dynamics. In such cases long time correlation due to sticky effects close to the invariant structures become important. It has been shown that such sticky effects lead to recurrence times statistics which obey a power-law decay [35].

ACKNOWLEDGMENTS

It is a pleasure to acknowledge support by the PROBRAL joint Brazilian-German program of CAPES (Brazil) and DAAD (Germany). M.W.B. thanks CNPq (Brazil) for financial support.

[1] R. Brown, Philosophical Magazine N. S. **4**, 161 (1828).
[2] A. Einstein, Ann. Phys. (Leipzig) **322**, 549 (1905).
[3] M. Smoluchowski, Ann. Phys. (Leipzig) **326**, 756 (1906).
[4] P. Langevin, Comptes Rendues Acad. Sci. **146**, 530 (1908).
[5] A. O. Caldeira and A. J. Leggett, Physica A **121**, 587 (1983).
[6] E. Cortés, B. J. West, and K. Lindenberg, J. Chem. Phys. **82**, 2708 (1985).
[7] S. T. Smith and R. Onofrio, Eur. Phys. J. B **61**, 271 (2008).
[8] L. Ratschbacher, C. Sias, L. Carcagni, J. M. Silver, C. Zipkes, and M. Kohl, Phys. Rev. Lett. **110**, 160402 (2013).

[9] K. W. Murch, S. J. Weber, C. Macklin, and I. Siddiqi, Nature **502**, 211 (2013).
[10] M. Sarovar, A. Ishizaki, G. R. Fleming, and K. B. Whaley, Nat. Phys. **6**, 462 (2010).
[11] P. Ullersma, Physica **32**, 27 (1966).
[12] J. Rosa and M. W. Beims, Physica A **342**, 29 (2004).
[13] J. Rosa and M. W. Beims, Physica A **386**, 54 (2007).
[14] J. Rosa and M. W. Beims, Phys. Rev. E **78**, 031126 (2008).
[15] C. Manchein, J. Rosa, and, M. W. Beims, Physica D **238**, 1688 (2009).
[16] Q. Wei, S. T. Smith, and R. Onofrio, Phys. Rev. E **79**, 031128 (2009).
[17] S. A. Abdulack, W. T. Strunz, and M. W. Beims, Phys. Rev. E **89**, 042141 (2014).
[18] T. O. de Carvalho and M. A. M. de Aguiar, Phys. Rev. Lett. **76**, 2690 (1996).
[19] M. Wilkinson, J. Phys. A: Math. Gen. **23**, 3603 (1990).
[20] M. V. Berry and J. M. Robbins, Proc. R. Soc. Lond. A **442**, 641 (1993).
[21] E. Ott, Phys. Rev. Lett. **42**, 1628 (1979).
[22] R. Brown, E. Ott, and C. Grebogi, Phys. Rev. Lett. **59**, 1173 (1987).
[23] C. Jarzynski, Phys. Rev. Lett. **74**, 2937 (1995).
[24] M. V. S. Bonança and M. A. M. de Aguiar, Physica A **365**, 333 (2006).
[25] J. D. Ramshaw, Phys. Lett. A **198**, 122 (1995).
[26] V. V. Flambaum and F. M. Izrailev, Phys. Rev. E **56**, 5144 (1997).
[27] F. Q. Potiguar and U. M. S. Costa, Physica A **342**, 145 (2004).
[28] M. A. Marchiori and M. A. M. de Aguiar, Phys. Rev. E **83**, 061112 (2011).
[29] A. B. Adib, J. Stat. Phys. **117**, 581 (2004).
[30] M. Bianucci, R. Mannella, B. J. West, and P. Grigolini, Phys. Rev. E **51**, 3002 (1995).
[31] R. Kubo, M. Toda, and N. Hashitsume, *Statistical Physics II* (Springer, Heidelberg, 1985).
[32] W. H. Press, S. A. Teukolsky, W. T. Vetterling, and B. P. Flannery, *Numerical Recipes in Fortran* (Cambridge University Press, Cambridge, MA, 1992).
[33] A. J. Lichtenberg and M. A. Lieberman, *Regular and Chaotic Dynamics* (Springer-Verlag, New York, 1992).
[34] A. Wolf, J. B. Swift, H. L. Swinney, and J. A. Vastano, Physica D **16**, 285 (1985).
[35] E. G. Altmann and H. Kantz, Phys. Rev. E **71**, 056106 (2005).